

## AN EFFICIENT METHOD TO IDENTIFY GALAXY CLUSTERS BY USING SUPERCOSMOS, 2MASS AND WISE DATA

W. W. XU<sup>1,2</sup>, Z. L. WEN<sup>1</sup> AND J. L. HAN<sup>1</sup>

*Draft version June 11, 2021*

### ABSTRACT

The survey data of Wide-field Infrared Survey Explorer (WISE) provide an opportunity for the identification of galaxy clusters. We present an efficient method for detecting galaxy clusters by combining the WISE data with SuperCOSMOS and 2MASS data. After performing star-galaxy separation, we calculate the number of companion galaxies around the galaxies with photometric redshifts previously estimated by the SuperCOSMOS, 2MASS and WISE data. A scaled richness is then defined to identify clusters. From a sky area of 275 deg<sup>2</sup> coincident with Sloan Digital Sky Survey Stripe 82 region, we identify 302 clusters in the redshift range of  $0.1 < z < 0.35$ , 247 (82%) of which are previously known SDSS clusters. The results indicate that our method is efficient for identifying galaxy clusters by using the all sky data of the SuperCOSMOS, 2MASS and WISE.

*Subject headings:* Infrared; Galaxy clusters; Redshifts

### 1. INTRODUCTION

Galaxy clusters are known as the largest gravitational bounded systems in the universe. They are located at nodes of cosmic web. The space distribution of galaxy clusters traces the large scale structure (Bahcall 1988; Allen et al. 2011; Hong et al. 2012). Their mass distribution can be used to constrain cosmological parameters (Reiprich & Bohringer 2002; Wen et al. 2010). Clusters are also regarded as natural gravitational lens to magnify faint background sources (Wen et al. 2011; Liang et al. 2013) and laboratories to study galaxy evolution (Wen & Han 2011; Liu et al. 2012). Discovery of galaxy clusters is the basis for many related studies.

In optical/infrared, a lot of methods have been used to detect clusters from image data. By visual inspection of optical images, Abell identified more than 4000 nearby rich clusters covering the whole sky (Abell 1958; Abell et al. 1989). Similar visual inspections were undertaken by Zwicky et al. (1968) and Gunn et al. (1986). For reducing subjectivity, automated peak-finding methods were developed, e.g., matched-filter algorithm (Postman et al. 1996), adaptive kernel technique (Gal et al. 2003) and Voronoi tessellation techniques (Ramella et al. 2001; Kim et al. 2002). The single-band image data always suffer severe contamination from foreground and background galaxies and provide very poor redshift estimation of clusters.

The Sloan Digital Sky Survey (SDSS, York et al. 2000) offers an opportunity to identify a large number of clusters. It provides photometry in five broad bands ( $u$ ,  $g$ ,  $r$ ,  $i$ , and  $z$ ) covering  $\sim 14,000$  deg<sup>2</sup>, as well as the follow-up spectroscopic observations. In such multi-band surveys, galaxy colors are related to their redshifts. Member galaxies have similar colors and show a red sequence, so that proper cuts in colors can reduce projection effect for cluster identification. A lot of red-sequence based methods have been developed (Gladders & Yee 2000, 2005; Goto et al. 2002; Koester et al. 2007). Photometric redshifts were estimated for all galaxies (Csabai et al. 2003; Oyaizu et al. 2008). A large number of galaxy clusters have been found based on photometric redshift (Wen et al. 2009, 2012; Szabo et al. 2011).

<sup>1</sup> National Astronomical Observatories, Chinese Academy of Sciences, Beijing 100012, China; zhonglue@nao.cas.cn

<sup>2</sup> University of Chinese Academy of Sciences, Beijing 100012, China

Except for Abell clusters at low redshift (Abell et al. 1989), there is no all sky cluster catalog up to intermediate redshift of  $z \sim 0.3$ . The Wide-field Infrared Survey Explorer (WISE) is an all-sky survey at infrared wavelengths with the observation depth similar to that of the SDSS (Yan et al. 2013), which provides an opportunity to identify many new clusters covering the whole sky. Combined with optical data, the WISE data have been used to identify clusters at high redshift (Gettings et al. 2012).

In this paper, we present a simple but very efficient method to identify galaxy clusters by combining the WISE data with the SuperCOSMOS (Hamby et al. 2001) and Two Micron All Sky Survey (2MASS, Skrutskie et al. 2006) data. In Section 2, we describe the data, present our method for the identification of galaxy clusters, and apply it to the data in the SDSS Stripe 82 region<sup>3</sup>. In Section 3, we compare the identified clusters with previous SDSS clusters. A summary is given in Section 4.

### 2. DATA AND ALGORITHM FOR CLUSTER IDENTIFICATION

2MASS is an all-sky survey in three infrared bands,  $J$  (1.25  $\mu\text{m}$ ),  $H$  (1.65  $\mu\text{m}$ ) and  $K_s$  (2.17  $\mu\text{m}$ ). The effective resolution of 2MASS is  $\sim 5''$ . The magnitude limits of 2MASS are 15.8, 15.1 and 14.3 (10 $\sigma$ ) for point sources, and 15.0, 14.3 and 13.5 for extended sources in the three bands, respectively (Skrutskie et al. 2006).

The WISE observes the whole sky in four infrared bands,  $W_1$  (3.4  $\mu\text{m}$ ),  $W_2$  (4.6  $\mu\text{m}$ ),  $W_3$  (12  $\mu\text{m}$ ) and  $W_4$  (22  $\mu\text{m}$ ). The angular resolutions in the four bands are 6.1'', 6.4'', 6.5'' and 12.0'', respectively. The all sky survey depths are 16.5, 15.5, 11.2 and 7.9 mag (5 $\sigma$ ) for point sources (Wright et al. 2010). The most important data for cluster identification are WISE  $W_1$ -band and 2MASS  $J$ -band magnitudes. In terms of detecting distant galaxies, the WISE data is much deeper than the 2MASS data. The limit of cluster detection mainly depends on the depth of the 2MASS data.

Because of the poor resolutions, both WISE and 2MASS data have no reliable star-galaxy separation for most objects by morphological parameters. However, stars and galaxies can be well separated by color index,  $W_1 - J$  (Kovács & Szapudi 2013). We cross-match the 2MASS-

<sup>3</sup> <http://cas.sdss.org/stripe82/en/>

WISE objects with known stars and galaxies in SDSS DR7 (Abazajian et al. 2009) brighter than  $r = 21$  mag with a matching radius of  $3''$ . In Figure 2, we show the efficiency for the star-galaxy separation with the  $W1 - J$  color index of the WISE-2MASS data. Galaxies are very well separated with the criteria of  $W1 - J < -1.5$  mag.

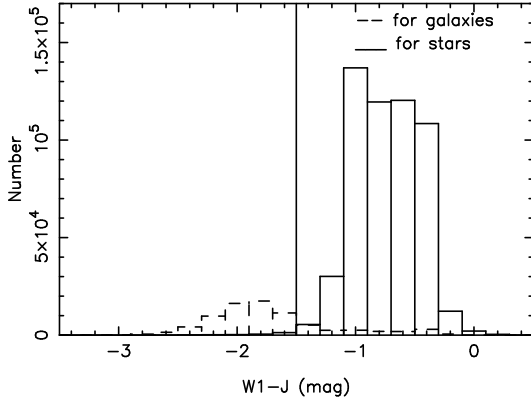


**Figure 1** Separation of stars and galaxies by color index,  $W1 - J$ . The vertical line is  $W1 - J = -1.5$  mag, which is used as the threshold for star-galaxy separation.

To get redshift information for galaxy clusters, we use the catalog of galaxy photometric redshifts<sup>4</sup> given by Bilicki et al. (2014) for 2MASS galaxies. By combining the data of SuperCOSMOS, 2MASS and WISE, these authors applied an artificial neural network approach to estimate photometric redshifts of galaxies covering the whole sky. The photometric redshift has an uncertainty of  $\sigma_z = 0.015$  and small percentage of outliers. Note that only 2MASS extended sources have photometric redshifts. The number of galaxies with photometric redshifts is about one tenth of the galaxies separated by  $W1 - J < -1.5$ .

Using the WISE-2MASS data together with photometric redshifts by Bilicki et al. (2014) in the SDSS Stripe 82 region of  $309^\circ \leq \text{RA} \leq 60^\circ$  and  $-1.25^\circ \leq \text{Dec} \leq 1.25^\circ$ , we make cluster identification in the following steps.

For each galaxy with a photometric redshift, we take it as the temporary central galaxy of a cluster candidate, and the photometric redshift is taken as the redshift of the cluster candidate. We then calculate the number of companion galaxies from all separated galaxies within a projected distance of 1 Mpc. The average number of background galaxies is estimated using the galaxies within the projected distance between 2 and 4 Mpc from the assumed central galaxy. We then get the net number of companion galaxies within 1 Mpc of the central galaxy after background subtraction, which is taken as a measured richness,  $R_{\text{mea}}$ . To avoid a cluster identified repeatedly, we applied the friend-of-friend technique (Huchra & Geller 1982) to merge the members into a cluster candidate, and consider only one cluster candidate within a projected distance of 1 Mpc and a photometric redshift difference of 0.05. We take the cluster candidate with the maximum measured richness,  $R_{\text{mea}}$ .

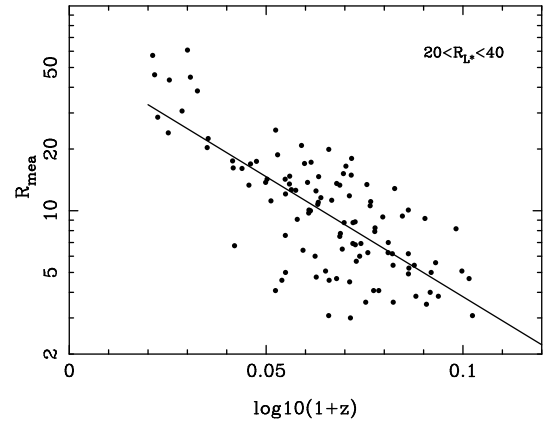


**Figure 2** The value of  $R_{\text{mea}}$  as a function of redshift for the matched WHL12 clusters of  $20 < R_{L*} < 40$ . The solid line is the best-fit relation.

The second step is to find a richness threshold to identify real galaxy clusters. The best selection is that the cluster richness is related to cluster mass. Because we use the flux-limited galaxy sample of the WISE-2MASS data, the measured richness,  $R_{\text{mea}}$ , strongly depends on redshift for clusters with a fixed mass. Here, we define a scaled richness with redshift correction,

$$R_{\text{scal}} = R_{\text{mea}} (1 + z)^\alpha, \quad (1)$$

to relate cluster mass, where  $\alpha$  is the correction slope. Note that the richness,  $R_{L*}$ , in the catalog of Wen et al. (2012, WHL12 hereafter) has a good correlation with cluster mass. Thus, we cross-match the identified cluster candidates with the WHL12 clusters of  $20 < R_{L*} < 40$  by using criteria of a projected separation of 1 Mpc and a redshift difference of 0.05. To get a proper value of  $\alpha$ , we plot  $R_{\text{scal}}$  as a function of redshift for the matched clusters (Figure 2). The best fit gives  $\alpha = 9.8 \pm 1.0$ . We get similar results when matching WHL12 clusters in other  $R_{L*}$  ranges. Figure 3 shows the comparison of  $R_{L*}$  with  $R_{\text{mea}}$  and  $R_{\text{scal}}$ . Clearly,  $R_{\text{scal}}$  has a better correlation with  $R_{L*}$  than with  $R_{\text{mea}}$ .

We define a cluster to have  $R_{\text{scal}} \geq 30$  in our new identifications. To avoid the occasional projection effect, we also require  $R_{\text{mea}} \geq 4$ . The cluster candidates with photometric redshift of  $z < 0.1$  are excluded because the angular radius varies rapidly for the fixed radius of 1 Mpc at low redshift, which induces large uncertainty on richness. Finally, we get 302 clusters in the redshift range of  $0.1 < z < 0.35$  from the  $275 \text{ deg}^2$  SDSS Stripe 82 area, which is listed in Table 1. The histograms for the redshift and scaled richness are shown in Figure 4. The identified clusters have a mean redshift of 0.18. If our algorithm is applied to the all sky SuperCOSMOS, 2MASS and WISE data excluding the Galactic plane of  $|b| > 10^\circ$ , we can find about 37,000 galaxy clusters, which will greatly enlarge the number of galaxy clusters in the region outside of the SDSS coverage.

<sup>4</sup> <http://surveys.roe.ac.uk/ssa/TWOMPZ>

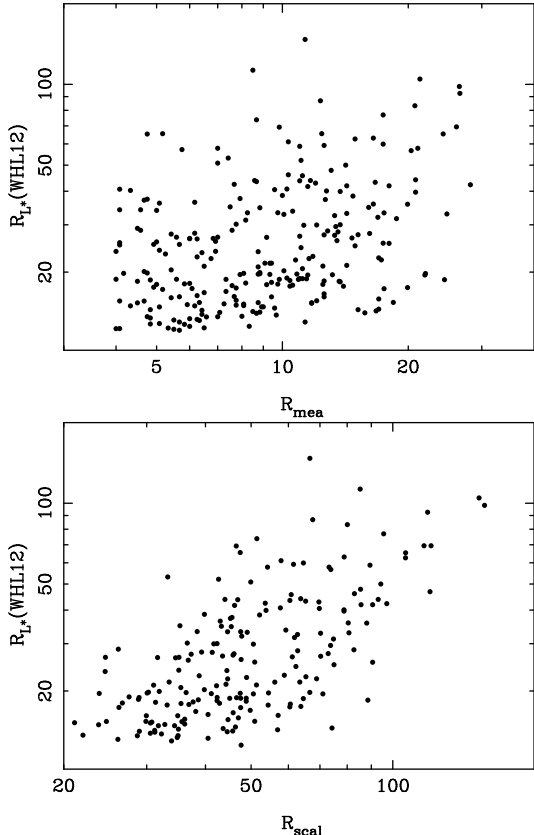


**Figure 3** Comparison of measured richness  $R_{\text{mea}}$  (upper panel) and scaled richness  $R_{\text{scal}}$  (lower panel) with the richness in WHL12 for matched cluster candidates.

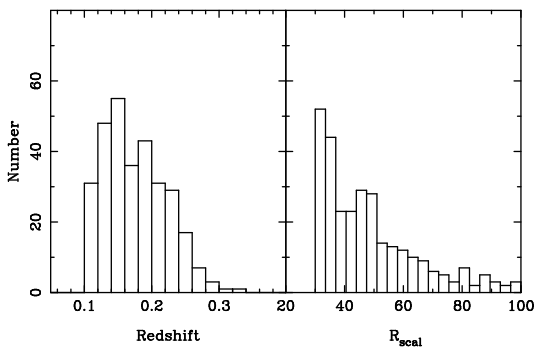


**Figure 4** Distributions of redshift and scaled richness for the 302 identified clusters.

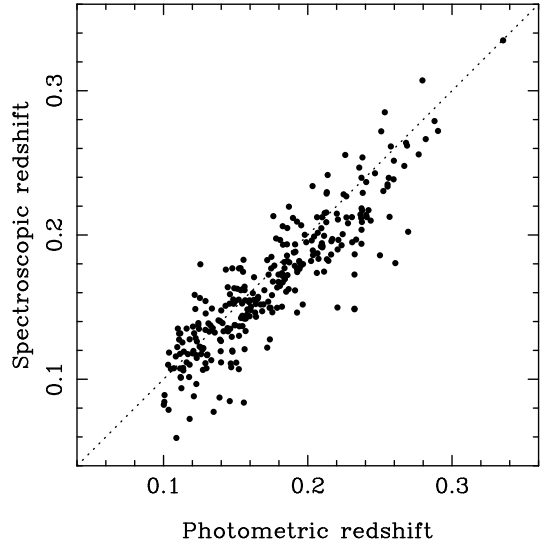


**Figure 5** Comparison between cluster photometric redshift and spectroscopic redshift for 291 clusters.

To estimate the uncertainty of photometric redshift of clusters, we compare the cluster redshifts with the spectroscopic redshifts of the central galaxies in the SDSS DR7 data (Abazajian et al. 2009). 291 of 302 central galaxies have their spectroscopic redshifts measured already. As shown in Figure 5, the cluster photometric redshift is consistent with spectroscopic redshift with a scatter of 0.022. The central galaxies without spectroscopic redshifts are not observed by the SDSS spectroscopic survey, probably due to fiber collision. We take the value of 0.022 as the typical uncertainty of cluster photometric redshift.

### 3. COMPARISON WITH PREVIOUS GALAXY CLUSTERS CATALOGS

There are many clusters in the Stripe 82 region identified previously in the catalogs (i.e., Goto et al. 2002; Koester et al. 2007; Hao et al. 2010; Szabo et al. 2011; Geach et al. 2011; Wen et al. 2009, 2012). Generally, these catalogs have a low false detection rate of  $\sim 5\%$ . The completeness is as high as  $> 90\%$  for clusters with mass  $> 1.0 \times 10^{14} M_\odot$  and is about 50% for cluster with mass  $0.6 \times 10^{14} M_\odot$  (e.g., Wen et al. 2012). We regard the clusters in these catalogs as true clusters and compare them with 302 identified clusters. 247 of 302 (82%) identified clusters are matched with the known clusters within a separation of 1 Mpc and a redshift difference of 0.05. The matched percentage of the identified clusters with known SDSS clusters varies with richness as expected, as shown in Figure 6. The matched percentage increases from 82% with a richness of  $R_{\text{scal}} \geq 30$  to 95% with a richness of  $R_{\text{scal}} \geq 60$ . Most of the unmatched clusters have a low richness which all previous methods are less sensitive to detect. In previous catalogs, the matched percentage between them is in the range of 40%–80%, and even lower for poor clusters with a small richness (Szabo et al. 2011; Wen et al. 2012). The value of 82% is very high compared with previous matched percentage, suggesting that our identification method is very efficient for finding clusters by using the SuperCOSMOS, 2MASS and WISE data.

There are 196 clusters matched with the WHL12 clusters, of which 118 (60%) have the central galaxies matched with the brightest cluster galaxies (BCG) of the WHL12, suggesting that the method presented in this paper has a high probability to find the BCGs. We calculate the projected distance

between the central galaxies of identified clusters and BCGs of the WHL12 clusters. As shown in Figure 7, the distribution is random for the central galaxies not matched with the BCGs. For these clusters, the BCGs may not be located at the positions with the maximum overdensity of galaxy numbers found within a radius of 1 Mpc. Some of these clusters may have multiple bright member galaxies in different sub-clusters.

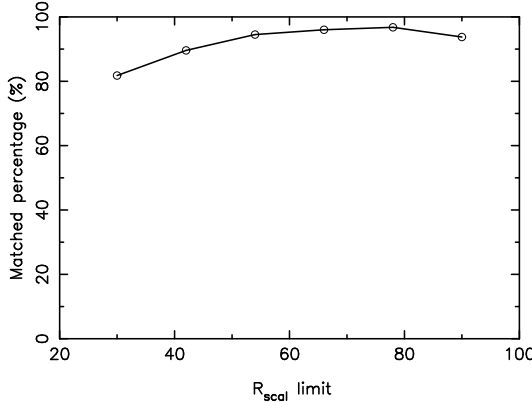


**Figure 6** Matched percentage of identified clusters by previously known SDSS clusters as a function of richness limit.

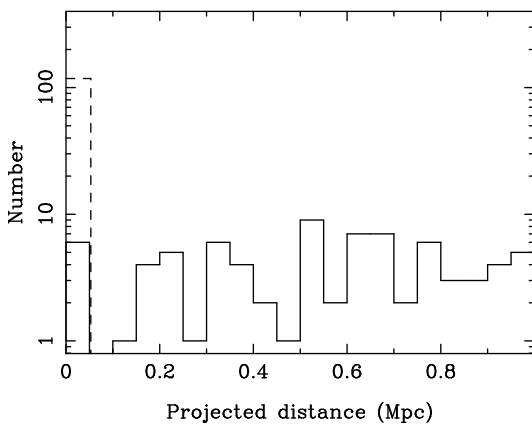


**Figure 7** Distribution of projected distance between central galaxies of the identified clusters and BCGs of the WHL12 clusters. The dashed line is for the matched central galaxies with angular offset less than 3'' from the BCGs.

Many works used red-sequence methods to identify clusters in multi-band surveys (e.g., Gladders & Yee 2000, 2005; Koester et al. 2007). The basis of such methods is that cluster galaxies have similar colors, which are tightly related to redshift. We check if the colors by the WISE and 2MASS data have tight correlations with redshift for the central galaxies. We find that the colors,  $J - W1$  and  $J - W3$ , have poor correlations with redshift (Figure 8). Cluster identification with  $J - W1$  and  $J - W3$  may have large uncertainty at redshift of  $z < 0.35$ . Therefore the photometric redshift data provide a better opportunity to identify a whole sky galaxy cluster catalog up to redshift  $z \sim 0.35$ .

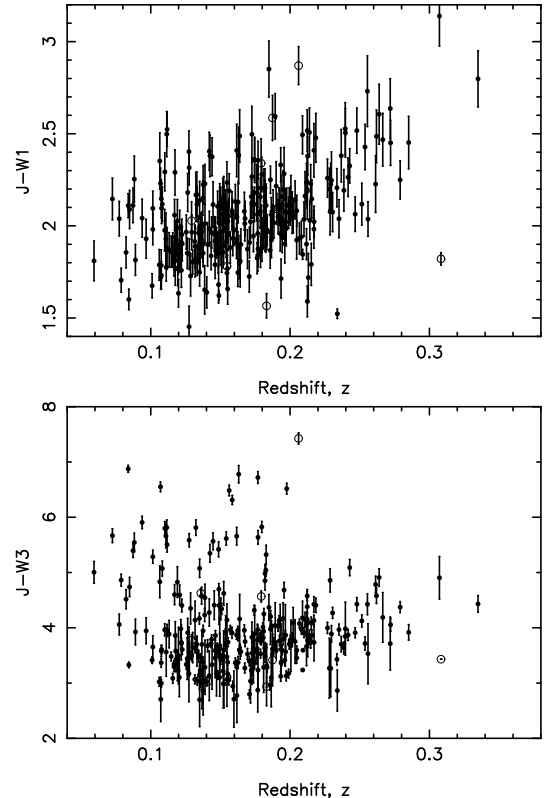


**Figure 8** Colors  $J - W1$  (upper panel) and  $J - W3$  (lower panel) of central galaxies versus cluster redshift. Black dots are for spectroscopic redshifts. Open circles are for photometric redshifts with a typical uncertainty of 0.022.

#### 4. SUMMARY

In this paper, we present an efficient method to identify galaxy clusters by using the SuperCOSMOS, 2MASS and WISE data. First, we perform star-galaxy separation by color index,  $W1 - J$ . Then, clusters are identified around the galaxies with estimated photometric redshift. We get a measured richness and define a scaled richness,  $R_{\text{scal}}$ , by comparing the richness of Wen et al. (2012). Our method is applied to the data in the SDSS Stripe 82 region and identify 302 clusters of  $R_{\text{scal}} \geq 30$  in the redshift range of  $0.1 < z < 0.35$ . The photometric redshift has an uncertainty of 0.022. 82% of our clusters are matched with previous SDSS cluster catalogs. Our results confirm that this approach has a good potential to detect many new galaxy clusters in the all sky data of SuperCOSMOS, 2MASS and WISE, especially in the region out of the SDSS coverage.

We thank the referee for valuable comments that helped to improve the paper. We thank Jun Han for carefully reading the manuscript, Zhongsheng Yuan and Jun Xu for useful discussion. The authors are supported by the National Natural Science Foundation (NNSF) of China (10833003 and 11103032) and the Young Researcher Grant of National Astronomical Observatories, Chinese Academy of Sciences. This publication makes use of data products from the Wide-field Infrared Survey Explorer, which is a joint project of the University of California, Los Angeles, and the Jet Propulsion Laboratory/California Institute of Technology, funded by the National Aeronautics and Space Administration. This research

has made use of the NASA/IPAC Infrared Science Archive, which is operated by the Jet Propulsion Laboratory, California Institute of Technology, under contract with the National Aeronautics and Space Administration. Funding for the SDSS and SDSS-II has been provided by the Alfred P. Sloan Foundation, the Participating Institutions, the National Science Foundation, the U.S. Department of Energy, the National Aeronautics and Space Administration, the Japanese Monbukagakusho, the Max Planck Society, and the Higher Education Funding Council for England. The SDSS Web site is <http://www.sdss.org/>. The SDSS is managed by the Astrophysical Research Consortium for the Participating Institutions. The Participating Institutions are the American Museum of Natural History, Astrophysical Institute Potsdam,

University of Basel, Cambridge University, Case Western Reserve University, University of Chicago, Drexel University, Fermilab, the Institute for Advanced Study, the Japan Participation Group, Johns Hopkins University, the Joint Institute for Nuclear Astrophysics, the Kavli Institute for Particle Astrophysics and Cosmology, the Korean Scientist Group, the Chinese Academy of Sciences (LAMOST), Los Alamos National Laboratory, the Max Planck Institute for Astronomy (MPIA), the Max Planck Institute for Astrophysics (MPA), New Mexico State University, Ohio State University, University of Pittsburgh, University of Portsmouth, Princeton University, the United States Naval Observatory, and the University of Washington.

## REFERENCES

- Abell, G. O. 1958, ApJS, 3, 211  
 Abell, G. O., Corwin, H. G., Jr., & Olowin, R. P. 1989, ApJS, 70, 1  
 Abazajian, K. N., Adelman-McCarthy, J. K., Agüeros, M. A., et al. 2009, ApJS, 182, 543  
 Allen, S. W., Evrard, A. E., & Mantz, A. B. 2011, ARA&A, 49, 409  
 Bahcall, N. A. 1988, ARA&A, 26, 631  
 Bilicki, M., Jarrett, T. H., Peacock, J. A., Cluver, M. E., & Steward, L. 2014, ApJS, 210, 9  
 Csabai, I., Budavári, T., Connolly, A. J., et al. 2003, AJ, 125, 580  
 Gal, R. R., de Carvalho, R. R., Lopes, P. A. A., et al. 2003, AJ, 125, 2064  
 Geach, J. E., Murphy, D. N. A., & Bower, R. G. 2011, MNRAS, 413, 3059  
 Gettings, D. P., Gonzalez, A. H., Stanford, S. A., et al. 2012, ApJ, 759, L23  
 Gladders, M. D., & Yee, H. K. C. 2000, AJ, 120, 2148  
 Gladders, M. D., & Yee, H. K. C. 2005, ApJS, 157, 1  
 Goto, T., Sekiguchi, M., Nichol, R. C., et al. 2002, AJ, 123, 1807  
 Gunn, J. E., Hoessel, J. G., & Oke, J. B. 1986, ApJ, 306, 30  
 Hambly, N. C., Irwin, M. J., & MacGillivray, H. T. 2001, MNRAS, 326, 1295  
 Hao, J., McKay, T. A., Koester, B. P., et al. 2010, ApJS, 191, 254  
 Hong, T., Han, J. L., Wen, Z. L., Sun, L., & Zhan, H. 2012, ApJ, 749, 81  
 Huchra, J. P., & Geller, M. J. 1982, ApJ, 257, 423  
 Kim, R. S. J., Kepner, J. V., Postman, M., et al. 2002, AJ, 123, 20  
 Koester, B. P., McKay, T. A., Annis, J., et al. 2007, ApJ, 660, 221  
 Kovács, A., & Szapudi, I. 2013, arXiv:1401.0156  
 Liang, S. M., Wen, Z. L., Han, J. L., & Jiang, Y. Y. 2014, Sci. China Phys. Mech. Astron., in press (arXiv:1310.4885)  
 Liu, F., Wen, Z., Han, J., & Meng, X. 2012, Science China Physics, Mechanics, and Astronomy, 55, 354  
 Oyaizu, H., Lima, M., Cunha, C. E., et al. 2008, ApJ, 674, 768  
 Postman, M., Lubin, L. M., Gunn, J. E., et al. 1996, AJ, 111, 615  
 Ramella, M., Boschin, W., Fadda, D., & Nonino, M. 2001, A&A, 368, 776  
 Reiprich, T. H., Böhringer, H. 2002, ApJ, 567, 716  
 Skrutskie, M. F., Cutri, R. M., Stiening, R., et al. 2006, AJ, 131, 1163  
 Szabo, T., Pierpaoli, E., Dong, F., Pipino, A., & Gunn, J. 2011, ApJ, 736, 21  
 Wen, Z. L., Han, J. L., & Liu, F. S. 2010, MNRAS, 407, 533  
 Wen, Z.-L., Han, J.-L., & Jiang, Y.-Y. 2011, Research in Astronomy and Astrophysics, 11, 1185  
 Wen, Z. L., & Han, J. L. 2011, ApJ, 734, 68  
 Wen, Z. L., Han, J. L., & Liu, F. S. 2009, ApJS, 183, 197  
 Wen, Z. L., Han, J. L., & Liu, F. S. 2012, ApJS, 199, 34  
 Wright, E. L., Eisenhardt, P. R. M., Mainzer, A. K., et al. 2010, AJ, 140, 1868  
 Yan, L., Donoso, E., Tsai, C.-W., et al. 2013, AJ, 145, 55  
 York, D. G., Adelman, J., Anderson, J. E., Jr., et al. 2000, AJ, 120, 1579  
 Zwicky, F., Herzog, E., & Wild, P. 1968, Pasadena: California Institute of Technology (CIT), 1961-1968,

TABLE 1  
THE 302 IDENTIFIED CLUSTER CANDIDATES IN THE STRIPE 82

ID	R.A. (deg)	Decl. (deg)	$z_p$ (4)	$z_s$ (5)	$J$ (mag) (6)	$W1$ (mag) (7)	$R_{scal}$ (8)	$R_{mea}$ (9)	Note (10)
(1)	(2)	(3)	(4)	(5)	(6)	(7)	(8)	(9)	(10)
1	312.7079	-1.0438	0.1335	0.1490	15.53 ± 0.10	13.52 ± 0.03	30.03	9.08	Geach
2	312.8900	-0.0495	0.1400	0.1477	15.15 ± 0.06	13.25 ± 0.02	41.98	12.08	MaxBCG,AMF,Geach,WHL12
3	313.0400	0.3102	0.1754	0.1464	15.55 ± 0.09	13.60 ± 0.03	33.57	7.42	MaxBCG,GMBCG,Geach,WHL12
4	314.3147	1.2120	0.1788	0.1636	15.61 ± 0.08	13.81 ± 0.03	36.30	7.83	New
5	315.0705	0.4328	0.1035	0.0788	15.39 ± 0.06	13.69 ± 0.03	40.71	15.50	New
6	315.7259	0.8867	0.2576	0.2614	16.45 ± 0.15	14.22 ± 0.04	83.93	10.33	AMF,Geach,WHL12
7	315.7609	0.8942	0.1340	0.1355	15.07 ± 0.07	13.12 ± 0.03	62.27	18.75	GMBCG,Geach,WHL12
8	315.8023	-1.0171	0.1912	0.1616	15.64 ± 0.08	13.73 ± 0.03	75.73	14.92	GMBCG,AMF,Geach,WHL12
9	315.8495	0.9987	0.1477	0.1769	16.06 ± 0.10	13.85 ± 0.04	36.20	9.83	WHL12
10	316.1830	0.9142	0.1826	0.1672	15.88 ± 0.10	13.80 ± 0.03	36.94	7.75	GMBCG,AMF,Geach,WHL12
11	317.9637	0.0149	0.2209	0.2107	16.18 ± 0.13	14.02 ± 0.03	43.97	7.00	MaxBCG,GMBCG,AMF,Geach,WHL12
12	318.5470	-0.5487	0.2553	0.2351	15.95 ± 0.10	13.91 ± 0.03	31.99	4.00	AMF,WHL12
13	319.3704	0.1176	0.2553	0.2336	16.05 ± 0.10	13.84 ± 0.03	33.35	4.17	MaxBCG,GMBCG,AMF,Geach,WHL12
14	319.5089	0.8675	0.1562	0.1208	15.72 ± 0.09	13.73 ± 0.03	36.30	9.25	Geach
15	319.9571	1.1862	0.1204	0.1365	15.52 ± 0.07	13.55 ± 0.02	49.88	16.67	AMF
16	320.9352	-0.6985	0.2308	0.1950	15.89 ± 0.10	13.69 ± 0.03	49.39	7.33	MaxBCG,GMBCG,AMF,Geach,WHL12
17	321.1893	-0.5187	0.2524	0.2305	15.98 ± 0.10	13.90 ± 0.04	54.87	7.00	MaxBCG,GMBCG,AMF,Geach,WHL12
18	321.4364	1.0129	0.1497	0.1374	15.54 ± 0.09	13.64 ± 0.03	65.10	17.42	GMBCG,AMF,Geach,WHL12
19	322.4165	0.0891	0.2033	0.2339	14.98 ± 0.99	13.46 ± 0.03	68.29	12.33	MaxBCG,GMBCG,Geach,WHL12
20	322.4345	0.3405	0.1952	0.1787	15.68 ± 0.10	13.52 ± 0.03	46.15	8.83	MaxBCG,Geach,WHL12
21	322.4928	-0.3298	0.1547	...	15.68 ± 0.09	13.90 ± 0.03	42.69	11.00	MaxBCG,GMBCG,Geach,WHL12
22	322.5165	-0.3523	0.2405	0.2367	16.37 ± 0.14	13.99 ± 0.03	50.52	7.00	MaxBCG,GMBCG,Geach,WHL12
23	322.5982	-0.0492	0.1569	0.1334	15.64 ± 0.07	13.82 ± 0.03	54.24	13.75	MaxBCG,GMBCG,Geach,WHL12
24	323.1762	1.1921	0.2061	...	16.11 ± 0.10	13.24 ± 0.02	37.72	6.67	New
25	323.5251	-0.5225	0.2381	0.2292	15.78 ± 0.11	13.55 ± 0.03	53.79	7.58	GMBCG,Geach
26	323.5826	0.5438	0.1967	0.1798	15.61 ± 0.07	13.73 ± 0.03	41.37	7.83	GMBCG,Geach
27	323.8004	-1.0496	0.3083	...	15.67 ± 0.99	13.85 ± 0.03	67.92	5.92	GMBCG,Geach,WHL12
28	323.9428	0.1158	0.1169	0.1174	15.81 ± 0.12	13.52 ± 0.03	120.70	41.42	Abell,MaxBCG,GMBCG,AMF,Geach,WHL12
29	324.6582	-0.3506	0.1521	0.1552	15.24 ± 0.07	13.58 ± 0.05	30.44	8.00	New
30	326.1441	1.1394	0.2267	0.2268	16.00 ± 0.10	13.74 ± 0.03	89.52	13.67	Abell,Geach,WHL12
31	326.3670	-0.7800	0.1850	0.1607	15.36 ± 0.09	13.23 ± 0.02	73.60	15.17	MaxBCG,GMBCG,Geach,WHL12
32	326.5361	-0.2424	0.2130	0.2287	16.15 ± 0.12	14.07 ± 0.04	31.67	5.33	Geach,WHL12
33	326.8617	0.7289	0.1181	0.0725	15.72 ± 0.11	13.57 ± 0.03	51.21	17.42	Abell,MaxBCG,Geach,WHL12
34	328.5980	0.0844	0.1603	0.1480	15.05 ± 0.08	12.94 ± 0.03	46.50	11.50	MaxBCG,GMBCG,Geach,WHL12
35	328.6150	0.6436	0.1831	...	14.86 ± 0.06	13.29 ± 0.03	31.11	6.50	Abell,MaxBCG,GMBCG,AMF,Geach,WHL12
36	328.7676	0.8724	0.2064	0.2123	16.14 ± 0.11	13.62 ± 0.03	58.51	10.33	GMBCG,AMF,Geach,WHL12
37	328.8372	1.1254	0.2370	0.2118	15.67 ± 0.08	13.77 ± 0.03	39.91	5.67	Geach,WHL12
38	328.9167	0.5372	0.1858	0.2048	15.51 ± 0.08	13.43 ± 0.03	46.75	9.58	MaxBCG,AMF,Geach,WHL12
39	329.3690	-0.9485	0.1273	0.1065	16.39 ± 0.15	14.04 ± 0.03	32.08	10.17	New
40	329.3874	-0.9288	0.2372	0.1939	15.74 ± 0.08	13.70 ± 0.03	71.06	10.08	MaxBCG,Geach,WHL12
41	329.9931	-0.6349	0.1108	0.1275	15.54 ± 0.10	14.09 ± 0.05	47.27	17.00	AMF,WHL12
42	330.1559	-0.5459	0.1398	0.1265	15.44 ± 0.10	13.26 ± 0.02	49.43	14.25	MaxBCG,Geach,WHL12
43	331.2684	-0.5626	0.1597	0.1437	15.73 ± 0.08	13.77 ± 0.03	69.46	17.25	MaxBCG,Geach,WHL12
44	331.6891	1.0279	0.2372	0.2397	16.25 ± 0.13	13.74 ± 0.03	43.50	6.17	AMF,Geach,WHL12
45	332.3338	1.2364	0.1606	0.1503	15.64 ± 0.09	13.67 ± 0.03	37.50	9.25	New
46	334.1963	-0.9939	0.1965	0.1518	15.78 ± 0.11	13.64 ± 0.03	31.64	6.00	WHL12
47	335.4678	-0.9728	0.3354	0.3349	16.51 ± 0.15	13.71 ± 0.03	65.23	4.75	Geach
48	335.4820	-1.0553	0.1051	0.1072	14.89 ± 0.06	13.17 ± 0.02	64.94	24.42	WHL12
49	335.5464	-1.0006	0.2206	0.1497	15.80 ± 0.09	13.92 ± 0.03	44.97	7.17	New
50	335.6234	0.5694	0.1859	0.1722	15.53 ± 0.09	13.37 ± 0.02	67.16	13.75	Abell,MaxBCG,Geach,WHL12
51	335.7316	0.5291	0.1445	0.1638	16.41 ± 0.14	13.92 ± 0.03	45.54	12.67	Abell,GMBCG,AMF,Geach,WHL12
52	336.0885	0.3597	0.1570	0.1420	15.71 ± 0.09	13.73 ± 0.03	65.81	16.67	MaxBCG,GMBCG,Geach,WHL12
53	336.2299	-0.3840	0.1559	0.1420	15.38 ± 0.10	12.98 ± 0.02	54.80	14.00	MaxBCG,Geach,WHL12
54	337.2881	0.4193	0.1523	0.1301	15.41 ± 0.06	13.61 ± 0.03	30.80	8.08	Geach,WHL12
55	337.5326	-0.0037	0.2279	0.2081	15.72 ± 0.08	13.78 ± 0.03	86.35	13.08	MaxBCG,GMBCG,AMF,Geach,WHL12
56	337.8498	0.2527	0.2769	0.2559	15.97 ± 0.09	13.93 ± 0.03	75.82	8.17	MaxBCG,GMBCG,Geach,WHL12
57	337.9117	-1.0345	0.1458	0.1524	15.94 ± 0.11	13.78 ± 0.03	31.46	8.67	New
58	338.4055	0.6970	0.1742	0.1495	15.99 ± 0.11	13.87 ± 0.03	56.38	12.58	AMF
59	338.5464	1.0411	0.1905	...	15.85 ± 0.08	13.76 ± 0.03	60.60	12.00	MaxBCG
60	338.8853	-1.1846	0.1007	0.0890	15.34 ± 0.08	13.52 ± 0.03	41.57	16.17	GMBCG,Geach,WHL12
61	339.5265	0.5325	0.2373	0.2036	15.89 ± 0.10	13.75 ± 0.03	34.71	4.92	WHL12
62	339.5725	-1.0250	0.1301	0.1167	15.43 ± 0.07	13.60 ± 0.03	64.22	19.92	MaxBCG,WHL12
63	339.6037	0.4290	0.1476	0.1199	15.58 ± 0.07	13.95 ± 0.03	36.79	10.00	GMBCG
64	339.6763	-0.4495	0.1737	0.1276	15.82 ± 0.09	13.50 ± 0.03	44.67	10.00	New
65	339.7389	0.9962	0.1241	0.1389	15.87 ± 0.10	13.86 ± 0.03	41.59	13.50	New

TABLE 1  
CONTINUED

ID	R.A. (deg)	Decl. (deg)	$z_p$	$z_s$	J (mag)	W1 (mag)	$R_{scal}$	$R_{mea}$	Note
(1)	(2)	(3)	(4)	(5)	(6)	(7)	(8)	(9)	(10)
66	339.7720	0.6534	0.2375	0.2090	15.60	13.76 ± 0.03	54.20	7.67	MaxBCG,Geach,WHL12
67	339.9143	1.1757	0.1641	0.1433	15.70 ± 0.07	13.86 ± 0.03	45.42	10.92	Geach,WHL12
68	340.6530	0.8837	0.1222	0.1286	15.65 ± 0.10	13.92 ± 0.04	50.59	16.67	New
69	340.8411	0.3386	0.1089	0.0593	15.78 ± 0.10	13.97 ± 0.04	46.78	17.08	WHL12
70	341.1638	0.5700	0.1137	0.1061	15.02 ± 0.08	13.23 ± 0.02	44.77	15.75	New
71	341.7559	0.9144	0.1793	...	15.81 ± 0.10	13.80 ± 0.03	34.92	7.50	MaxBCG,Geach
72	342.0809	-0.6117	0.2099	0.2123	15.90 ± 0.08	13.70 ± 0.03	46.02	7.92	GMBCG,AMF,WHL12
73	342.1753	0.9131	0.1359	...	15.13 ± 0.08	13.15 ± 0.03	38.73	11.50	MaxBCG,AMF
74	342.5280	0.8538	0.1927	0.1743	15.68 ± 0.09	13.56 ± 0.03	47.87	9.33	MaxBCG,GMBCG,AMF,Geach,WHL12
75	342.7946	-0.7928	0.2365	0.2142	15.92 ± 0.10	13.89 ± 0.03	38.59	5.50	Geach,WHL12
76	342.9160	1.1677	0.1388	0.0873	15.65 ± 0.09	13.54 ± 0.03	30.98	9.00	New
77	343.9557	0.5725	0.1910	0.1786	15.85 ± 0.09	13.77 ± 0.03	35.07	6.92	New
78	344.0618	-0.5811	0.1032	0.1100	15.93 ± 0.11	13.95 ± 0.03	81.27	31.00	Abell,MaxBCG,GMBCG,AMF,Geach,WHL12
79	344.1515	-0.4658	0.1469	0.1083	15.55 ± 0.09	13.43 ± 0.03	74.41	20.33	Abell,MaxBCG,GMBCG,AMF,Geach,WHL12
80	344.3402	-1.1362	0.1792	...	15.82 ± 0.13	13.48 ± 0.03	38.00	8.17	MaxBCG,Geach,WHL12
81	344.5970	0.2678	0.1291	0.1542	15.89 ± 0.09	13.85 ± 0.03	57.84	18.08	MaxBCG,WHL12
82	344.6125	-0.1018	0.1872	0.1810	15.72 ± 0.09	13.74 ± 0.03	54.62	11.08	MaxBCG,Geach
83	344.6595	0.5849	0.1252	0.1563	15.67 ± 0.09	13.48 ± 0.03	32.60	10.50	New
84	344.7387	1.2057	0.1085	0.1158	15.38 ± 0.09	13.51 ± 0.03	47.80	17.50	New
85	345.0132	1.1510	0.1304	0.1171	15.73 ± 0.08	13.67 ± 0.03	40.63	12.58	New
86	345.0288	0.2221	0.1874	...	15.62 ± 0.12	13.03 ± 0.02	62.11	12.58	GMBCG,AMF,Geach,WHL12
87	345.0460	0.3640	0.2248	0.2282	15.70 ± 0.11	13.50 ± 0.03	35.00	5.42	WHL12
88	345.5182	0.2212	0.1293	...	15.79 ± 0.10	13.76 ± 0.03	33.39	10.42	MaxBCG,GMBCG,Geach,WHL12
89	345.9451	0.7804	0.1566	0.1547	15.84 ± 0.11	13.60 ± 0.03	39.66	10.08	MaxBCG
90	348.1483	0.1520	0.1260	0.1174	15.03 ± 0.08	13.09 ± 0.03	44.52	14.25	MaxBCG,Geach,WHL12
91	350.2303	0.5441	0.2067	0.1873	15.73 ± 0.09	13.71 ± 0.03	62.91	11.08	MaxBCG,Geach,WHL12
92	350.6064	1.0693	0.1396	0.1194	15.09 ± 0.08	13.32 ± 0.04	30.30	8.75	CE,MaxBCG,AMF,Geach,WHL12
93	350.7556	0.8997	0.1269	0.1205	15.21 ± 0.07	13.39 ± 0.03	41.43	13.17	MaxBCG,AMF,WHL12
94	351.0899	0.3193	0.1735	0.1495	15.11 ± 0.08	12.99 ± 0.03	88.83	19.92	Abell,CE,MaxBCG,GMBCG,AMF,Geach,WHL12
95	351.1997	0.9442	0.1038	0.1185	15.22 ± 0.08	13.30 ± 0.03	30.94	11.75	CE,WHL12
96	354.4262	0.3038	0.1207	0.1196	15.17 ± 0.07	13.36 ± 0.03	77.26	25.75	Abell
97	355.0894	0.2696	0.1447	0.1332	15.38 ± 0.09	13.26 ± 0.02	32.41	9.00	CE
98	355.2489	0.0817	0.1748	0.1848	15.66 ± 0.15	12.81 ± 0.03	119.64	26.58	Abell,CE,MaxBCG,GMBCG,AMF,Geach,WHL12
99	355.9156	0.4243	0.2500	0.1859	15.66 ± 0.07	13.41 ± 0.02	50.10	6.50	New
100	356.0726	-0.8548	0.2607	0.1805	15.87 ± 0.08	13.91 ± 0.03	33.87	4.08	New
101	356.5196	-0.1857	0.2818	0.2665	16.45 ± 0.14	13.98 ± 0.03	48.76	5.08	CE,MaxBCG,GMBCG,AMF,Geach,WHL12
102	356.5763	0.9610	0.1355	0.1324	16.06 ± 0.12	13.89 ± 0.03	32.48	9.67	Geach,WHL12
103	356.8651	-0.1538	0.2681	0.2639	16.63 ± 0.16	14.02 ± 0.03	35.66	4.08	CE,GMBCG,AMF,Geach,WHL12
104	358.7088	-0.1407	0.1808	0.1966	15.82 ± 0.08	13.82 ± 0.03	36.48	7.75	WHL12
105	359.8242	0.3167	0.1181	0.1101	16.01 ± 0.10	13.72 ± 0.03	31.60	10.75	New
106	0.1008	-1.2457	0.1562	0.1618	15.26 ± 0.07	13.21 ± 0.03	32.69	8.33	New
107	0.2157	-1.1984	0.2170	0.1972	15.66 ± 0.09	13.68 ± 0.03	30.55	5.00	New
108	0.3598	-0.0288	0.2669	0.2479	16.21 ± 0.12	13.69 ± 0.03	49.82	5.75	CE,MaxBCG,GMBCG,AMF,Geach,WHL12
109	1.1300	-1.1274	0.1768	0.1788	15.82 ± 0.08	13.96 ± 0.03	35.78	7.83	New
110	1.8501	-0.7548	0.2325	0.1866	15.94 ± 0.09	14.02 ± 0.03	51.15	7.50	CE,Geach
111	1.9482	-0.7442	0.1522	0.1070	15.67 ± 0.08	13.44 ± 0.03	34.92	9.17	WHL12
112	2.1160	-0.0048	0.1216	0.1585	15.45 ± 0.07	13.38 ± 0.03	33.75	11.17	New
113	2.4194	0.4251	0.1904	0.1878	15.74 ± 0.09	13.64 ± 0.03	35.32	7.00	CE,Geach,WHL12
114	3.0125	-1.0070	0.1459	0.0848	15.71 ± 0.10	13.62 ± 0.03	33.60	9.25	New
115	3.1982	0.7877	0.1581	0.1484	15.60 ± 0.10	13.75 ± 0.04	40.10	10.08	MaxBCG,WHL12
116	3.2122	0.2891	0.1430	0.1509	16.03 ± 0.10	14.17 ± 0.04	47.98	13.50	CE,MaxBCG,GMBCG,AMF,WHL12
117	3.3711	0.6735	0.1006	0.0843	14.98 ± 0.05	13.38 ± 0.02	34.88	13.58	CE
118	4.1540	-0.5023	0.1393	0.1402	15.40 ± 0.08	13.76 ± 0.03	44.66	12.92	CE
119	4.2262	-1.0625	0.2098	0.1943	15.43 ± 0.08	13.49 ± 0.03	30.02	5.17	CE,MaxBCG,GMBCG,AMF,Geach,WHL12
120	4.2529	-1.2286	0.1536	0.1617	15.54 ± 0.08	13.61 ± 0.03	47.79	12.42	GMBCG,AMF,WHL12
121	4.4067	-0.8784	0.2306	0.2124	16.42 ± 0.15	14.23 ± 0.03	95.39	14.17	CE,MaxBCG,GMBCG,AMF,Geach,WHL12
122	4.6355	-0.7675	0.2102	0.1924	15.85 ± 0.09	13.75 ± 0.03	48.02	8.25	CE,MaxBCG,GMBCG,Geach,WHL12
123	5.0673	0.0794	0.2409	0.2124	15.21 ± 0.06	13.62 ± 0.06	154.31	21.33	MaxBCG,GMBCG,AMF,Geach,WHL12
124	5.0890	-0.2531	0.2436	0.2100	15.75 ± 0.09	13.71 ± 0.03	70.66	9.58	MaxBCG,AMF,Geach,WHL12
125	5.1726	-1.1764	0.1989	0.1950	15.83 ± 0.10	13.80 ± 0.03	37.14	6.92	MaxBCG,Geach,WHL12
126	5.2040	0.1822	0.2405	0.2139	16.31 ± 0.13	13.80 ± 0.03	107.68	14.92	MaxBCG,GMBCG,WHL12
127	5.3191	-0.8368	0.1115	0.1075	15.40 ± 0.08	13.61 ± 0.03	117.18	41.92	Abell,CE,MaxBCG,GMBCG,Geach,WHL12
128	5.3476	-0.8259	0.1797	0.1675	15.40 ± 0.09	13.39 ± 0.03	121.72	26.08	CE,MaxBCG,GMBCG,AMF,Geach
129	5.6779	-0.6892	0.1867	0.1625	15.74 ± 0.07	13.99 ± 0.03	37.24	7.58	MaxBCG,Geach,WHL12
130	5.7616	-0.1367	0.1726	0.1538	15.90 ± 0.11	13.91 ± 0.03	107.41	24.25	Abell,CE,MaxBCG,AMF,Geach,WHL12

TABLE 1  
CONTINUED

ID	R.A. (deg)	Decl. (deg)	$z_p$	$z_s$	$J$ (mag)	$W1$ (mag)	$R_{scal}$	$R_{mea}$	Note
(1)	(2)	(3)	(4)	(5)	(6)	(7)	(8)	(9)	(10)
131	6.1235	-1.0774	0.1311	0.1387	15.99 ± 0.12	14.34 ± 0.05	30.58	9.42	Geach
132	6.3241	-0.7247	0.1511	0.1627	15.78 ± 0.11	13.65 ± 0.03	30.51	8.08	CE,MaxBCG,GMBCG,Geach,WHL12
133	6.6855	1.2357	0.1673	0.1518	15.58 ± 0.10	13.52 ± 0.03	49.33	11.58	Geach,WHL12
134	7.1900	-0.0595	0.1761	0.2131	16.01 ± 0.12	14.29 ± 0.05	52.29	11.50	CE,MaxBCG,GMBCG,AMF,Geach,WHL12
135	7.2203	-0.2431	0.1504	0.1115	15.98 ± 0.12	13.48 ± 0.03	57.92	15.42	CE
136	7.2757	0.8811	0.1131	0.1255	15.36 ± 0.09	13.39 ± 0.03	30.65	10.83	New
137	7.4465	0.4922	0.2091	0.1921	15.91 ± 0.09	13.80 ± 0.03	48.12	8.33	WHL12
138	8.0469	-0.6669	0.2201	0.2148	16.08 ± 0.10	13.85 ± 0.03	79.63	12.75	CE,MaxBCG,AMF,Geach,WHL12
139	8.5832	0.8158	0.2035	0.1893	16.23 ± 0.12	13.64 ± 0.03	96.65	17.42	CE,MaxBCG,GMBCG,AMF,Geach,WHL12
140	8.7574	-1.2049	0.1897	0.2118	15.94 ± 0.10	13.71 ± 0.03	59.40	11.83	CE,Geach,WHL12
141	8.7992	0.7300	0.2688	0.2620	16.47 ± 0.14	13.98 ± 0.03	49.00	5.58	CE,GMBCG,Geach,WHL12
142	8.8420	1.0672	0.2101	0.1914	15.83 ± 0.09	13.78 ± 0.03	31.98	5.50	Geach,WHL12
143	9.2985	0.0967	0.2260	0.2555	16.44 ± 0.19	13.71 ± 0.03	83.61	12.83	Geach,WHL12
144	9.6975	-1.1918	0.1954	0.2067	15.93 ± 0.08	14.00 ± 0.03	49.31	9.42	CE,WHL12
145	9.7217	-0.2841	0.1858	0.1820	15.86 ± 0.10	13.65 ± 0.03	47.97	9.83	CE
146	9.9280	0.6277	0.1926	0.1462	15.76 ± 0.08	13.84 ± 0.03	30.35	5.92	New
147	9.9306	-0.9176	0.1072	0.1076	15.95 ± 0.10	13.80 ± 0.03	43.49	16.08	CE,WHL12
148	10.8143	0.2296	0.2117	0.2152	15.97 ± 0.11	14.18 ± 0.03	41.65	7.08	MaxBCG,GMBCG
149	10.8270	-0.3129	0.1545	0.1525	15.15 ± 0.08	13.02 ± 0.02	37.77	9.75	CE,Geach
150	10.8951	0.1760	0.1693	0.1519	15.43 ± 0.08	13.57 ± 0.03	86.85	20.08	Geach
151	10.8962	0.10196	0.2164	0.1957	15.91 ± 0.14	13.63 ± 0.03	56.77	9.33	CE,GMBCG,AMF,Geach,WHL12
152	11.0052	0.1145	0.1869	0.2171	16.19 ± 0.14	13.78 ± 0.04	81.20	16.50	CE,MaxBCG,GMBCG,AMF,Geach,WHL12
153	11.0195	1.0314	0.1160	0.1117	15.43 ± 0.09	12.91 ± 0.02	43.90	15.17	Geach,WHL12
154	11.0375	1.1917	0.1478	0.1191	15.76 ± 0.11	13.73 ± 0.04	46.37	12.58	WHL12
155	11.1551	-0.9223	0.2242	0.2006	15.95 ± 0.12	13.80 ± 0.03	39.69	6.17	CE,MaxBCG,GMBCG,Geach,WHL12
156	11.3335	0.7793	0.1466	0.1109	16.13 ± 0.13	14.20 ± 0.05	34.97	9.58	New
157	11.3770	-0.7964	0.1684	0.1472	15.10 ± 0.08	13.19 ± 0.03	47.26	11.00	Abell,CE,MaxBCG,GMBCG,Geach,WHL12
158	11.5601	0.0004	0.1399	0.1117	15.88 ± 0.11	14.00 ± 0.03	97.81	28.17	CE,MaxBCG,GMBCG,AMF,Geach,WHL12
159	11.5934	-0.1551	0.2373	0.2185	16.15 ± 0.13	13.67 ± 0.03	61.17	8.67	CE,MaxBCG,Geach,WHL12
160	11.8588	-0.9482	0.1523	0.1768	15.86 ± 0.08	14.02 ± 0.03	79.39	20.83	Abell,CE
161	12.9848	-1.0960	0.1290	0.1342	15.20 ± 0.09	13.24 ± 0.03	35.70	11.17	MaxBCG,AMF,WHL12
162	13.4089	0.9207	0.2534	0.2851	16.17 ± 0.14	13.72 ± 0.03	61.19	7.75	CE,MaxBCG,AMF,Geach,WHL12
163	13.4427	-0.7802	0.1241	0.1376	15.39 ± 0.10	13.17 ± 0.03	64.17	20.83	Abell,CE,GMBCG,Geach,WHL12
164	13.8141	-0.3482	0.1635	0.1462	15.44 ± 0.07	13.65 ± 0.03	51.77	12.50	CE,MaxBCG,GMBCG,Geach,WHL12
165	14.3250	0.0257	0.1912	0.1935	15.75 ± 0.11	13.59 ± 0.03	54.97	10.83	CE,Geach,WHL12
166	15.2043	-0.4221	0.2696	0.2022	15.86 ± 0.09	13.81 ± 0.03	60.31	6.83	New
167	15.2281	-1.1552	0.1412	...	15.00 ± 9.99	13.90 ± 0.03	47.60	13.58	New
168	15.3084	0.5743	0.2113	0.1994	15.63 ± 0.09	13.52 ± 0.03	70.42	12.00	CE,MaxBCG,GMBCG,AMF,Geach,WHL12
169	15.3301	-0.0553	0.1856	0.1935	15.47 ± 0.09	13.76 ± 0.05	56.85	11.67	CE
170	15.3609	-0.0636	0.1136	0.1078	14.90 ± 0.08	12.80 ± 0.02	48.06	16.92	Abell,CE,Geach,WHL12
171	15.3715	-0.2619	0.2234	0.1929	15.71 ± 0.09	13.75 ± 0.03	36.26	5.67	WHL12
172	15.3876	0.5376	0.1114	0.1176	15.38 ± 0.09	13.61 ± 0.03	35.13	12.58	WHL12
173	15.4146	-0.2248	0.1290	0.1111	15.56 ± 0.07	13.78 ± 0.03	50.59	15.83	Abell,CE,WHL12
174	15.4679	0.6898	0.1292	0.1456	15.94 ± 0.09	13.98 ± 0.03	30.16	9.42	CE,WHL12
175	15.6797	1.1362	0.1546	0.1440	15.41 ± 0.10	13.03 ± 0.02	65.92	17.00	CE,MaxBCG,Geach,WHL12
176	15.7192	0.2479	0.2094	0.2047	15.79 ± 0.10	13.87 ± 0.03	61.22	10.58	CE,Geach,WHL12
177	16.0185	-0.4345	0.2879	0.2790	16.04 ± 0.10	13.79 ± 0.03	46.72	4.67	CE,MaxBCG,GMBCG,Geach,WHL12
178	16.2306	0.0602	0.2903	0.2721	16.24 ± 0.12	13.79 ± 0.03	86.44	8.50	CE,MaxBCG,GMBCG,Geach,WHL12
179	16.6342	0.6310	0.1578	0.1447	16.13 ± 0.12	14.01 ± 0.03	38.73	9.75	WHL12
180	16.8165	0.6614	0.1496	0.1541	15.55 ± 0.08	13.64 ± 0.03	37.97	10.17	CE
181	16.8618	0.1470	0.2597	0.2515	16.11 ± 0.11	13.99 ± 0.03	46.03	5.58	CE,MaxBCG,AMF,Geach,WHL12
182	16.9189	1.0481	0.1483	0.1553	15.52 ± 0.10	13.49 ± 0.03	31.44	8.50	WHL12
183	17.3901	-0.8986	0.2063	0.1737	15.45 ± 0.08	13.51 ± 0.03	59.87	10.58	CE,Geach,WHL12
184	17.4051	-0.9297	0.1210	0.0882	16.16 ± 0.12	13.91 ± 0.04	59.65	19.83	New
185	17.6656	1.0666	0.1926	0.1764	15.44 ± 0.08	13.61 ± 0.03	44.86	8.75	CE,MaxBCG,AMF,WHL12
186	17.9198	-0.7625	0.1116	0.1318	15.79 ± 0.11	13.90 ± 0.03	43.14	15.42	Geach,WHL12
187	17.9535	-0.0181	0.2379	0.2538	15.89 ± 0.12	13.46 ± 0.03	97.41	13.75	CE,MaxBCG,GMBCG,Geach,WHL12
188	18.1542	-0.6651	0.2357	0.2467	15.85 ± 0.09	13.79 ± 0.03	52.88	7.58	MaxBCG,Geach
189	18.2290	1.0638	0.1416	0.1333	15.62 ± 0.07	13.81 ± 0.03	34.01	9.67	New
190	18.2797	-0.0010	0.2128	0.2156	15.99 ± 0.10	13.84 ± 0.03	30.13	5.08	Geach,WHL12
191	18.5621	-0.9125	0.2074	0.1835	15.56 ± 0.08	13.58 ± 0.03	55.63	9.75	CE,MaxBCG,GMBCG,Geach,WHL12
192	18.6568	-0.8458	0.2023	0.1820	15.94 ± 0.09	13.98 ± 0.03	61.46	11.17	GMBCG,AMF,WHL12
193	18.8958	-0.4914	0.1554	0.1828	15.98 ± 0.11	13.87 ± 0.04	35.77	9.17	Geach,WHL12
194	19.1019	-0.1334	0.1943	0.1766	15.45 ± 0.09	13.39 ± 0.03	45.84	8.83	CE,MaxBCG,Geach,WHL12
195	19.4654	-1.2269	0.2377	0.2171	15.97 ± 0.10	13.99 ± 0.03	37.13	5.25	Geach,WHL12

TABLE 1  
CONTINUED

ID	R.A. (deg)	Decl. (deg)	$z_p$ (4)	$z_s$ (5)	$J$ (mag) (6)	$W1$ (mag) (7)	$R_{scal}$ (8)	$R_{mea}$ (9)	Note (10)
196	19.7274	-1.0984	0.1276	0.1216	$15.02 \pm 0.07$	$13.18 \pm 0.03$	35.83	11.33	New
197	19.7734	-1.2336	0.1260	0.1220	$15.21 \pm 0.08$	$13.45 \pm 0.05$	55.45	17.75	New
198	19.8598	-0.7436	0.2421	0.2172	$15.68 \pm 0.08$	$13.66 \pm 0.03$	39.56	5.42	CE,MaxBCG,Geach,WHL12
199	19.8798	-1.1572	0.2036	0.1860	$16.07 \pm 0.11$	$14.10 \pm 0.03$	74.52	13.42	CE,Geach,WHL12
200	20.1750	-0.6050	0.1124	0.0938	$15.88 \pm 0.10$	$13.84 \pm 0.03$	37.53	13.33	WHL12
201	20.4632	-0.1918	0.1979	0.2001	$15.69 \pm 0.10$	$13.58 \pm 0.03$	31.96	6.00	CE,AMF,Geach,WHL12
202	20.4820	0.0662	0.1347	0.0774	$15.24 \pm 0.09$	$13.20 \pm 0.03$	32.29	9.67	New
203	20.5108	0.3345	0.1551	0.1745	$15.53 \pm 0.11$	$13.17 \pm 0.03$	80.74	20.75	Abell,CE,MaxBCG,GMBCG,AMF,Geach,WHL12
204	20.6525	-0.8140	0.1797	0.1726	$15.65 \pm 0.10$	$13.38 \pm 0.03$	63.38	13.58	CE,MaxBCG,GMBCG,AMF,Geach,WHL12
205	20.8281	1.1489	0.1298	0.1076	$15.80 \pm 0.07$	$14.07 \pm 0.03$	35.12	10.92	New
206	21.0764	-1.2405	0.1728	0.1725	$15.56 \pm 0.08$	$13.43 \pm 0.02$	51.02	11.50	GMBCG,Geach,WHL12
207	21.2476	-0.8441	0.1627	0.1707	$15.68 \pm 0.08$	$13.95 \pm 0.03$	32.61	7.92	New
208	21.5269	1.2269	0.1925	0.2093	$15.48 \pm 9.99$	$14.56 \pm 0.05$	35.45	6.92	CE,AMF,Geach,WHL12
209	21.7496	-0.7839	0.1807	0.1647	$15.66 \pm 0.08$	$13.76 \pm 0.03$	31.37	6.67	New
210	23.2450	0.9407	0.1250	0.1226	$15.38 \pm 0.09$	$13.48 \pm 0.03$	42.62	13.75	CE,MaxBCG,Geach,WHL12
211	23.7048	-0.6121	0.1557	0.0838	$15.10 \pm 0.06$	$12.99 \pm 0.03$	38.10	9.75	CE,GMBCG,AMF,Geach,WHL12
212	23.7313	0.3878	0.1592	0.1535	$15.74 \pm 0.11$	$13.66 \pm 0.03$	40.13	10.00	MaxBCG,AMF,Geach,WHL12
213	23.7849	-1.1513	0.1649	0.1555	$15.73 \pm 0.08$	$13.78 \pm 0.03$	44.98	10.75	CE,GMBCG,Geach,WHL12
214	23.8864	0.3775	0.1486	0.1523	$15.66 \pm 0.10$	$13.77 \pm 0.03$	34.93	9.42	Geach
215	23.9820	0.5584	0.1160	0.1351	$15.33 \pm 0.07$	$13.58 \pm 0.03$	33.28	11.50	New
216	24.3334	0.9561	0.1780	0.1976	$15.85 \pm 0.09$	$13.74 \pm 0.03$	46.46	10.08	New
217	24.7484	-0.8523	0.1202	0.1179	$15.53 \pm 0.09$	$13.61 \pm 0.03$	44.34	14.83	New
218	24.8218	0.3343	0.2212	0.1966	$15.97 \pm 0.12$	$13.89 \pm 0.03$	36.21	5.75	New
219	25.2334	0.1560	0.1758	0.1677	$15.58 \pm 0.09$	$13.54 \pm 0.03$	51.02	11.25	CE,Geach,WHL12
220	25.3794	-0.9283	0.1596	0.1547	$15.60 \pm 0.08$	$13.86 \pm 0.03$	36.89	9.17	CE,Geach
221	25.4900	-1.1074	0.1653	0.1560	$15.20 \pm 0.09$	$13.15 \pm 0.02$	46.18	11.00	CE,MaxBCG,AMF,Geach,WHL12
222	25.6666	0.1151	0.1120	0.1010	$15.44 \pm 0.06$	$13.77 \pm 0.03$	33.44	11.92	New
223	25.6991	0.8671	0.1118	0.1015	$15.61 \pm 0.09$	$13.52 \pm 0.03$	31.76	11.33	New
224	25.7110	0.7474	0.2027	0.1962	$15.81 \pm 0.10$	$13.91 \pm 0.03$	35.41	6.42	CE,WHL12
225	26.2515	-0.8150	0.2335	0.1968	$15.95 \pm 0.10$	$13.93 \pm 0.03$	50.36	7.33	CE,WHL12
226	26.3010	-0.0931	0.2044	0.1989	$15.48 \pm 0.08$	$13.41 \pm 0.03$	34.91	6.25	CE,GMBCG,Geach,WHL12
227	26.6881	-0.6752	0.1002	0.0823	$15.51 \pm 0.08$	$13.65 \pm 0.03$	44.83	17.50	AMF,WHL12
228	27.0689	0.3583	0.1826	0.2061	...	$13.92 \pm 0.03$	50.05	10.50	CE
229	27.7459	-1.0235	0.1752	0.1583	$15.93 \pm 0.10$	$13.85 \pm 0.03$	36.90	8.17	Geach
230	27.8014	-0.9955	0.2466	0.2428	$16.07 \pm 0.09$	$13.74 \pm 0.03$	57.76	7.67	CE,WHL12
231	28.1525	-0.2279	0.1746	0.1768	$15.39 \pm 0.08$	$13.43 \pm 0.02$	32.96	7.33	New
232	28.1750	1.0072	0.2132	0.2297	$16.07 \pm 0.15$	$13.82 \pm 0.04$	67.37	11.33	Abell,CE,MaxBCG,GMBCG,AMF,Geach,WHL12
233	28.1897	-0.3932	0.1534	0.1770	$15.68 \pm 0.09$	$13.81 \pm 0.03$	43.52	11.33	New
234	28.2245	-0.8960	0.1141	0.1192	$15.17 \pm 0.09$	$13.27 \pm 0.03$	50.87	17.83	New
235	28.2534	-0.5705	0.1317	0.1331	$16.04 \pm 0.12$	$13.87 \pm 0.03$	71.54	21.92	CE,MaxBCG,WHL12
236	28.3570	-1.1600	0.2138	0.2416	$15.85 \pm 0.10$	$13.59 \pm 0.03$	158.35	26.50	Abell,CE,MaxBCG,GMBCG,AMF,Geach,WHL12
237	29.1181	1.0605	0.1719	0.1826	$15.64 \pm 0.08$	$13.70 \pm 0.03$	140.27	31.83	New
238	29.3485	0.4178	0.1462	0.1350	$15.07 \pm 0.07$	$13.18 \pm 0.02$	32.15	8.83	CE,MaxBCG,GMBCG,Geach,WHL12
239	29.4308	-0.1504	0.1246	0.1349	$15.85 \pm 0.10$	$13.95 \pm 0.04$	38.89	12.58	MaxBCG,GMBCG,Geach,WHL12
240	29.4772	-0.6338	0.1914	0.1884	$15.97 \pm 0.08$	$13.95 \pm 0.03$	91.52	18.00	Abell,CE,GMBCG,AMF,Geach,WHL12
241	29.4970	-0.7244	0.2162	0.1865	$15.78 \pm 0.09$	$13.72 \pm 0.03$	86.56	14.25	Abell,CE,MaxBCG,GMBCG,AMF,Geach,WHL12
242	29.7756	0.8355	0.1443	0.1354	$15.58 \pm 0.08$	$13.73 \pm 0.03$	32.01	8.92	Geach,WHL12
243	29.8175	-0.1096	0.1626	0.1550	$15.61 \pm 0.07$	$13.84 \pm 0.03$	46.98	11.42	CE,MaxBCG,Geach,WHL12
244	30.0376	-0.8842	0.2128	0.2089	$16.18 \pm 0.10$	$13.69 \pm 0.03$	38.55	6.50	WHL12
245	30.3347	-0.4569	0.1619	0.1597	$15.45 \pm 0.08$	$13.47 \pm 0.02$	33.07	8.08	CE,MaxBCG,GMBCG,AMF,Geach,WHL12
246	30.5012	-0.4818	0.1460	0.1589	$15.71 \pm 0.09$	$13.78 \pm 0.03$	40.60	11.17	Geach
247	31.0914	-0.8329	0.1526	0.1367	$15.54 \pm 0.08$	$13.63 \pm 0.03$	30.24	7.92	New
248	31.1257	0.3046	0.2324	0.1726	$16.25 \pm 0.15$	$13.75 \pm 0.03$	64.19	9.42	Abell,CE,MaxBCG,AMF,Geach,WHL12
249	31.1304	0.2282	0.1490	0.1631	$16.26 \pm 0.15$	$13.88 \pm 0.04$	33.76	9.08	CE,MaxBCG,Geach,WHL12
250	31.1345	-1.0540	0.1699	0.1617	$16.23 \pm 0.14$	$13.82 \pm 0.03$	43.44	10.00	CE,Geach
251	31.3167	0.0574	0.1331	0.1132	$15.75 \pm 0.09$	$13.88 \pm 0.03$	49.47	15.00	New
252	31.3794	0.1897	0.1826	0.1716	$15.37 \pm 0.09$	$13.35 \pm 0.02$	30.17	6.33	CE,MaxBCG,AMF,Geach,WHL12
253	31.4742	0.0331	0.1821	0.1735	$15.42 \pm 0.07$	$13.30 \pm 0.03$	63.33	13.33	Geach,WHL12
254	32.4464	-0.1118	0.1639	0.1521	$15.54 \pm 0.09$	$13.52 \pm 0.03$	36.70	8.83	CE,Geach,WHL12
255	32.5758	-0.10184	0.1842	0.1709	$15.66 \pm 0.08$	$13.75 \pm 0.03$	79.58	16.50	Abell,CE,MaxBCG,AMF,Geach,WHL12
256	32.7266	-1.1567	0.1432	0.1760	$15.86 \pm 0.15$	$13.68 \pm 0.03$	52.52	14.75	CE,Geach,WHL12
257	32.8846	0.1167	0.2268	0.2122	$16.57 \pm 0.14$	$14.33 \pm 0.03$	40.96	6.25	CE,MaxBCG,GMBCG,Geach,WHL12
258	33.0959	-0.4210	0.1177	0.1015	$15.37 \pm 0.08$	$13.39 \pm 0.02$	32.49	11.08	Geach
259	33.1749	0.4748	0.2069	0.2015	$15.91 \pm 0.11$	$13.84 \pm 0.03$	58.30	10.25	CE,MaxBCG,AMF,Geach,WHL12
260	33.4638	0.4673	0.1940	0.1820	$15.79 \pm 0.11$	$13.66 \pm 0.03$	44.43	8.58	CE,MaxBCG,GMBCG,AMF,Geach,WHL12

TABLE 1  
CONTINUED

ID	R.A. (deg)	Decl. (deg)	$z_p$	$z_s$	$J$ (mag)	$W1$ (mag)	$R_{scal}$	$R_{mea}$	Note
(1)	(2)	(3)	(4)	(5)	(6)	(7)	(8)	(9)	(10)
261	33.4849	0.5268	0.2567	0.2126	15.91 ± 0.10	13.53 ± 0.03	94.30	11.67	CE,MaxBCG,GMBCG,AMF,Geach,WHL12
262	33.5527	-0.1887	0.1381	0.1408	15.59 ± 0.11	13.69 ± 0.04	57.35	16.75	CE,MaxBCG,GMBCG,AMF,Geach,WHL12
263	33.7983	1.0014	0.1095	0.1223	15.18 ± 0.08	13.23 ± 0.02	43.37	15.75	CE
264	33.7986	0.9053	0.1719	0.1219	15.96 ± 0.09	14.05 ± 0.03	74.92	17.00	New
265	34.6748	0.1138	0.2509	0.2719	16.30 ± 0.16	13.66 ± 0.03	71.14	9.17	CE,MaxBCG,GMBCG,AMF,Geach,WHL12
266	36.3090	-1.0862	0.1841	0.1694	15.70 ± 0.10	13.83 ± 0.03	31.32	6.50	CE,GMBCG,Geach,WHL12
267	36.7314	-1.0641	0.1227	0.0967	15.63 ± 0.10	13.70 ± 0.03	47.97	15.75	New
268	37.3373	0.5937	0.1108	0.1316	15.12 ± 0.08	13.20 ± 0.03	51.22	18.42	WHL12
269	37.7454	1.1128	0.1787	0.1495	15.61 ± 0.09	13.52 ± 0.03	49.79	10.75	CE
270	38.4721	0.0777	0.1856	0.1857	15.30 ± 0.09	13.43 ± 0.04	42.63	8.75	CE,Geach,WHL12
271	40.2131	-0.9324	0.2561	0.2396	16.31 ± 0.14	13.78 ± 0.03	40.21	5.00	CE,MaxBCG,AMF,Geach,WHL12
272	40.6842	-0.9660	0.1255	0.1797	15.64 ± 0.09	13.36 ± 0.03	31.91	10.25	MaxBCG
273	40.8013	-1.0201	0.2595	0.2386	15.86 ± 0.11	13.67 ± 0.03	90.60	11.00	CE,GMBCG,AMF,Geach,WHL12
274	41.4178	-0.7229	0.2143	0.1821	15.65 ± 0.09	13.54 ± 0.03	51.98	8.67	CE,MaxBCG,GMBCG,AMF,Geach,WHL12
275	41.8485	0.1005	0.1944	0.1810	15.33 ± 0.07	13.29 ± 0.03	35.49	6.83	Geach,WHL12
276	42.3182	-0.7739	0.1493	0.1376	15.13 ± 0.07	13.28 ± 0.02	45.02	12.08	WHL12
277	42.3603	0.0250	0.1821	0.1503	15.55 ± 0.10	13.44 ± 0.02	35.63	7.50	CE,MaxBCG,GMBCG,AMF,Geach,WHL12
278	42.4043	0.2698	0.1839	0.1770	15.95 ± 0.10	13.59 ± 0.03	30.91	6.42	New
279	42.9448	-0.1646	0.2133	0.1832	15.62 ± 0.09	13.66 ± 0.03	34.69	5.83	Geach,WHL12
280	43.1920	1.0847	0.1325	0.1374	15.42 ± 0.09	13.27 ± 0.02	81.28	24.75	CE,Geach,WHL12
281	44.7325	0.2605	0.1181	0.1277	15.53 ± 0.08	13.68 ± 0.03	51.21	17.42	WHL12
282	44.8857	0.2318	0.1828	0.1933	15.30 ± 0.09	12.97 ± 0.02	46.93	9.83	CE,MaxBCG,GMBCG,AMF,Geach,WHL12
283	45.6562	-0.6689	0.2207	0.1900	16.23 ± 0.13	14.01 ± 0.03	39.23	6.25	CE,Geach,WHL12
284	45.7460	-0.1935	0.1656	0.1571	15.48 ± 0.08	13.60 ± 0.03	61.70	14.67	CE,MaxBCG,AMF,Geach,WHL12
285	46.0997	0.8304	0.1099	0.1351	15.92 ± 0.10	13.78 ± 0.03	32.91	11.92	New
286	46.1983	-0.9336	0.1550	0.1626	15.72 ± 0.08	13.84 ± 0.03	32.73	8.42	New
287	46.6213	0.9996	0.1493	0.1536	15.59 ± 0.08	13.54 ± 0.02	30.75	8.25	CE,Geach
288	47.2143	-1.1733	0.1231	0.1262	15.50 ± 0.08	13.65 ± 0.02	31.57	10.33	Geach
289	48.3834	0.9172	0.1537	0.1425	16.16 ± 0.11	13.78 ± 0.03	34.66	9.00	CE,WHL12
290	48.5910	-0.5879	0.1228	0.1167	15.66 ± 0.08	13.85 ± 0.03	67.06	22.00	MaxBCG,AMF,Geach,WHL12
291	48.6184	0.2598	0.1473	0.1294	15.81 ± 0.09	13.85 ± 0.03	46.17	12.58	CE,Geach,WHL12
292	49.3038	0.1131	0.1230	0.1147	15.06 ± 0.08	13.20 ± 0.03	35.88	11.75	WHL12
293	49.7007	0.6802	0.2113	0.1746	16.37 ± 0.12	14.01 ± 0.03	35.21	6.00	CE,WHL12
294	50.1673	-1.2419	0.1836	0.1812	16.03 ± 0.10	13.82 ± 0.03	30.83	6.42	CE,Geach,WHL12
295	50.5087	1.1235	0.2324	0.1489	15.33 ± 9.99	13.71 ± 0.03	32.91	4.83	CE,Geach
296	50.7242	0.7819	0.1220	0.1487	15.73 ± 0.09	14.05 ± 0.04	33.84	11.17	CE,Geach
297	52.9716	-0.7835	0.1547	0.1368	15.34 ± 0.07	13.34 ± 0.02	43.00	11.08	CE,GMBCG,AMF,Geach,WHL12
298	53.5507	1.1746	0.1562	0.1642	15.63 ± 0.13	13.82 ± 0.05	49.72	12.67	CE,Geach
299	53.6419	-1.1646	0.1409	0.1389	15.43 ± 0.10	13.20 ± 0.03	73.76	21.08	CE,GMBCG,Geach,WHL12
300	54.9725	-0.2834	0.1392	0.1274	15.44 ± 0.11	13.04 ± 0.03	43.17	12.50	WHL12
301	55.6778	-0.2856	0.2795	0.3072	16.60 ± 0.16	13.46 ± 0.03	58.30	6.17	CE,MaxBCG,GMBCG,AMF,Geach,WHL12
302	58.2873	-0.8459	0.1212	0.1319	15.59 ± 0.09	13.77 ± 0.03	34.11	11.33	WHL12

Note. Column(1): the sequence number; Column(2): R.A. (J2000) of cluster center in degree; Column(3): Decl. (J2000) of cluster center in degree; Column(4): photometric redshift of cluster with a typical uncertainty of 0.022; Column(5): spectroscopic redshift of central galaxy with a typical uncertainty of  $2 \times 10^{-4}$ ; Column(6):  $J$ -band magnitude of central galaxy; Column(7):  $W1$ -band magnitude of central galaxy; Column(8): scaled richness of cluster; Column(9): measured richness of cluster. Column(10): Notes for known clusters in other catalogs: Abell (Abell 1958; Abell et al. 1989); CE (Goto et al. 2002); MaxBCG (Koester et al. 2007); GMBCG (Hao et al. 2010); AMF (Szabo et al. 2011); Geach (Geach et al. 2011), WHL12 (Wen et al. 2012); newly identified clusters are labelled “New”.